Flow Unit Perspective on Room Temperature Homogeneous Plastic Deformation in Metallic Glasses

Z. Lu, W. Jiao, W. H. Wang, and H. Y. Bai*
Institute of Physics, Chinese Academy of Sciences, Beijing 100190, China
(Received 30 November 2013; published 25 July 2014)

A mandrel winding method, which can realize remarkable homogeneous plastic deformation at room temperature for various metallic glasses, is applied to characterize plastic flow units and study their relationship with macroscopic deformations and relaxations. The method can provide information on the activation energy, activation time, size, intrinsic relaxation time, distribution, and density of flow units. We find the plasticity of a metallic glass can be controlled through modulating the features of flow units. The results have benefits for better understanding the structural origins of deformations and relaxations, and for designing metallic glasses with improved performances.

DOI: 10.1103/PhysRevLett.113.045501 PACS numbers: 62.20.F-, 61.43.Dq, 81.05.Kf

Metallic glasses (MGs) have diverse and unique mechanical properties and great application potentials [1–7]. Nevertheless, the underlying structural origin for their unique and wide spectrum of mechanical properties, especially the in-depth intrinsic deformation mechanisms of MGs, remains unclear [7–13] because the relationship between their atomic-level structure and the mechanical properties is difficult to characterize. Argon [14] introduced the shear transformation zones model and regarded the shear transformation zones as a kind of reversible flow unit for deformations in MGs. Computer simulations and experiments also show that liquidlike regions in MGs with the viscoelasticity flow feature act as the flow units, accommodating the deformation and initiating the shear banding [15,16]. Recently, the liquidlike regions in glass have been directly imaged by aberration-corrected transmission electron microscopy [17]. These flow units can be activated and percolated by applied stress or elevated temperature, inducing the global plasticity or relaxations of MGs [18,19]. On the other hand, the basic physics of relaxations, including β relaxation, which is the source of the localized atomic mobility in the glass state and has practical significance to many features and properties of glasses [10], is found to be closely related to the flow units and the Poisson's ratio, and obvious β relaxation is an indicator of the abundant flow units in a MG [10,18–27]. The finding enables insights into the relaxation mechanism of mechanical response of MGs. However, due to the disordered random structure and brittleness features of MGs, probing the characteristics of flow units as well as their evolution and percolation during deformation and relaxations remains a challenge. The correlations among flow units, deformations, relaxations, and mechanical properties of MGs are unclear.

In this Letter, a mandrel winding method, which can realize a pronounced homogeneous plastic deformation at room temperature (RT) for various MGs, is applied to investigate the characterization of flow units as well as their relationships with plastic deformations and relaxations in MGs. The found microstructural information on flow units has potential benefits for a better understanding of the deformation and relaxation mechanisms and the brittle-to-ductile transition, and for the design of MGs with improved performances.

Metallic glassy ribbons with a uniform thickness of 50 μm, distinctly different mechanical behaviors, and glass transition temperatures T_g were prepared using a melt-spinning technique (For details of the ribbons' preparation and their structure characterization, see Supplemental Material and Table S1 [28]). The β relaxations were tested using a dynamical mechanical analyzer (DMA, TA Q800; see Supplemental Material and Fig. S1 [28]). The ribbons were deformed by winding them at RT around an oxide glassy rod with a diameter of 5.3 mm (the mandrel). Each ribbon was wound about the mandrel in one of two methods, either helically [Fig. 1(a)] or scrolled like a clockwork spring [Fig. 1(b)]. The fully wound states were mechanically constrained for a period of time t (the holding time), and then released from the mandrel. The minimum curvature radius r of the released ribbon was measured to estimate its residual strain ε. To study flow units using this method, we varied the holding time t, and used ribbons with different relaxation behaviors, features, treatment conditions, and mechanical behaviors.

As an example, Fig. 1(c) shows a picture of a released $La_{75}Ni_{7.5}Al_{16}Co_{1.5}$ ribbon which was helically wound and then held in place around the mandrel at RT for 24 h. Clearly, the ribbon was plastically deformed into a helical shape, and the released ribbon displays no significant recovery from the induced deformation strain even after several months, as shown in Fig. 1(d) and Fig. S2 [28]. This indicates that the significant plastic deformation in the MG was induced at RT by the mandrel winding method. The SEM image [Fig. 1(e)] shows no shear bands on either

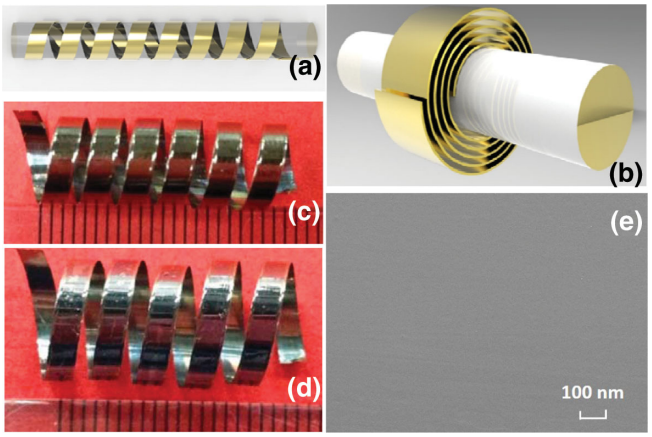

FIG. 1 (color). (a) A schematic illustration of the helical mandrel winding and (b) the clockwork spring winding methods. (c) An image of the released $La_{75}Ni_{7.5}Al_{16}Co_{1.5}$ ribbon after helically winding and holding in place for 24 h. (d) A picture of the released ribbon after 40 d, showing no significant residual strain recovery. (e) A SEM picture of the surface topography of the coiled MG showing no shear bands.

surface of the deformed ribbons, confirming that the pronounced deformation is homogenous. XRD patterns show that the deformation does not cause crystallization (Fig. S3 [28]). We also annealed the unconstrained coiled ribbon at $0.8T_g$ for 2 h. As shown in Fig. S4 [28], the ribbon maintains its coiled shape and has no observable recovery, further confirming the permanent plastic strain in the MG induced by the mandrel winding method.

We estimate the homogenous plastic deformation strain ε (or residual strain) induced by the winding method with [26]

$$\varepsilon = d/2r, \tag{1}$$

where d is the thickness of the ribbon and r is the minimum curvature radius of the released ribbon. The details of the derivation of Eq. (1) are presented in the Supplemental Material [28]. All the ribbons were subjected to an initial imposed strain of 0.943%. The r and ε of the deformed ribbons which were fully wound and then held in place for 24 h are listed in Table S1. The ε of $La_{75}Ni_{7.5}Al_{16}Co_{1.5}$, after winding and holding for 24 h, is ~0.6%, and a larger homogenous plastic strain can be obtained by extending the holding time of the wound state. As long as a sufficiently long holding time is applied, almost all kinds of MG ribbons we studied, including Zr-, Fe-, Mg-, Al-, and rare earth-based MG ribbons can be homogeneously and plastically deformed by the mandrel method. For example, a $Zr_{65}Cu_{17.5}Ni_{10}Al_{7.5}$ ribbon was homogeneously plastically deformed by this method by holding it wound for 720 h (see Fig. S5 [28]).

We attribute this homogeneous deformability to the activation of the flow units and the delocalization of strain in the MG. This is in sharp contrast with the shear banding mode as usually observed in MGs, which results in disappointingly low plasticity of MGs at RT [1–8]. The nanoscale localized flow units are liquidlike zones which have higher energy, higher mobility, and lower elastic moduli as compared to those of the matrix, and are more prone to shear under applied stresses [10,18,19]. Brittleness as an intrinsic defect of MGs hinders precise study on some fundamental issues such as deformation, relaxation, and dynamic evolutions, for which large plasticity is needed for statistical analysis [1–8]. The pronounced homogeneous deformation at RT for the various MGs obtained by the winding method permits accurate study of the flow unit, its activation and characteristics, and its relation to the deformations.

To study the relationship between the activation energy of the flow units E_{FU} and plastic deformation using the winding method, we chose a series of MGs with different T_g (The values of T_g of $Ce_{70}Al_{10}Ni_{10}Cu_{10}$, $Ce_{68}Al_{20}Cu_{10}Co_2$, $La_{68}Al_{20}Cu_{10}Co_2$, $La_{75}Ni_{7.5}Al_{16}Co_{1.5}$, $La_{60}Al_{20}Co_{20}$, $Pd_{40}Ni_{10}Cu_{30}P_{20}$ are 368, 396, 413, 415, 464, and 569 K, respectively). The E_{FU} is roughly related to T_g by [10] $E_{FU} \approx 26RT_g$, where R is the gas constant, so the flow units in a MG with higher T_g are more difficult to be activated. Figures 2(a)–2(b) show a comparison of the various coiled MGs after winding and holding in place for 24 h using the clockwork spring winding method. Clearly, the $Ce_{70}Al_{10}Ni_{10}Cu_{10}$ with the lowest T_g and E_{FU} has the smallest curvature radius r and the highest residual strain ε, and the $Pd_{40}Ni_{10}Cu_{30}P_{20}$, which has the highest T_g, has insignificant plastic deformation. With increasing T_g or E_{FU}, the r of these coiled ribbons increases, and their residual strain ε decreases as shown in Fig. 2(c). These results confirm that the plastic deformation is closely related to E_{FU}, and the MG system with a lower E_{FU} can be more readily deformed homogeneously.

The T_g of $La_{68}Al_{20}Cu_{10}Co_2$ is only slightly lower than that of $La_{75}Ni_{7.5}Al_{16}Co_{1.5}$, but they had significantly different ε when they were deformed in the same conditions by the mandrel winding method. This indicates that the deformation could not be associated solely with T_g or E_{FU}. It is found that the β relaxation of $La_{75}Ni_{7.5}Al_{16}Co_{1.5}$ is much stronger than that of $La_{68}Al_{20}Cu_{10}Co_2$ (see Fig. S6 [28]). We then study the relation between deformation and β relaxation, which is also related to the density of the flow units in MGs [10]. To manipulate the β relaxation behavior or the density of the flow units, we annealed the as-cast $La_{75}Ni_{7.5}Al_{16}Co_{1.5}$ ribbon at $0.8T_g$ (330 K) for 15, 30, 60, and 120 min, respectively. The MGs retain their glassy structure and their T_g alteration is insignificant after annealing (see Figs. S7–S8 [28]). The change of the loss modulus (E'') [normalized by the maximum peak value of the storage modulus (E')] induced by the annealing is given in Fig. 3(a). The β-relaxation peak intensity decreases with an increase in annealing time, demonstrating a decrease in the density of flow units with an extended annealing [29,30]. We fully wound the as-cast and annealed ribbons

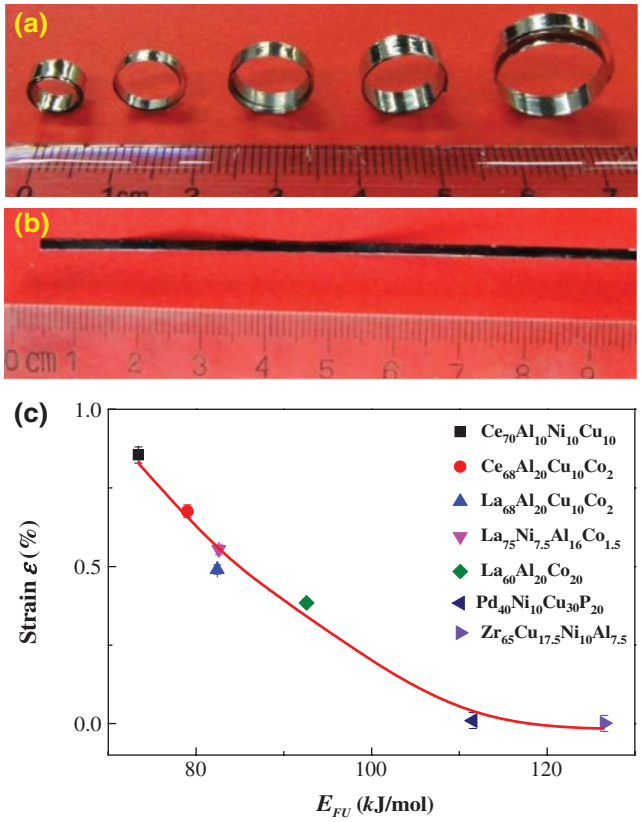

FIG. 2 (color). (a) From left to right, the released $Ce_{70}Al_{10}Ni_{10}Cu_{10}$, $Ce_{68}Al_{20}Cu_{10}Co_2$, $La_{75}Ni_{7.5}Al_{16}Co_{1.5}$, $La_{68}Al_{20}Cu_{10}Co_2$, $La_{60}Al_{20}Co_{20}$, and (b) $Pd_{40}Ni_{10}Cu_{30}P_{20}$ ribbons, which were mandrel wound and held for 24 h. (c) The residual strain ε vs the activation energy of flow units (the solid line is a guide for the eye) for these ribbons.

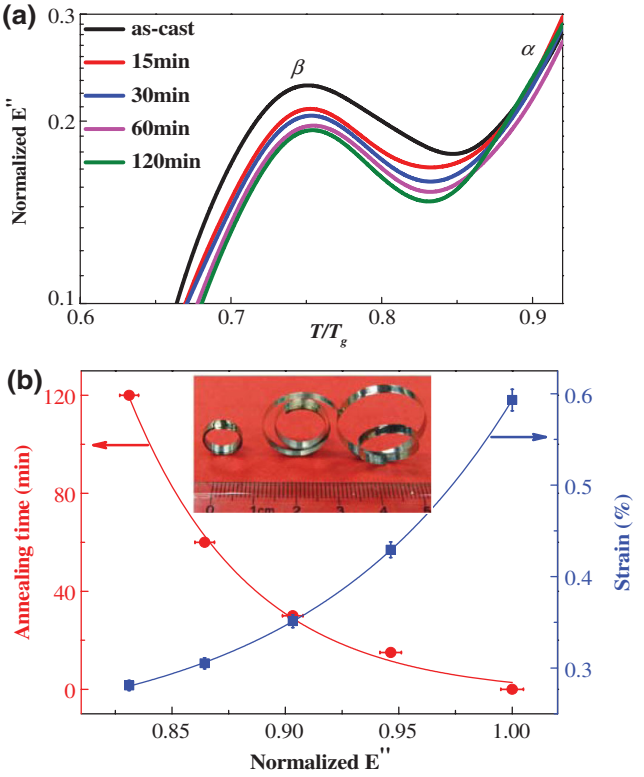

FIG. 3 (color). (a) The intensity of β relaxations of $La_{75}Ni_{7.5}Al_{16}Co_{1.5}$ gradually reduces with an increase of annealing time. (b) The relationship between ε, annealing time, and the intensity of β relaxation (normalized by the β-relaxation peak height of as-cast ribbon). The inset is the picture of coiled MGs which were annealed (from left to right) for 0, 15, and 30 min before imposing mandrel winding, respectively.

at RT and held for 24 h, and the changes in ε, the annealing time, and the normalized β-relaxation intensity of the annealed MGs are shown in Fig. 3(b), and the inset is the picture of these coiled annealed ribbons. The ε decreases with the attenuation of the intensity of β relaxation, which coincides with a decrease in the density of flow units [1,10,18,25,31]. The results indicate that the activation of high density of flow units can readily lead to the percolation of flow units or macroscopic plastic deformation in MGs.

According to the elastic model, the E_{FU} in MGs is determined by elastic moduli which are time dependent [2,32]. The activation of flow units and the plasticity of the MG could therefore be time dependent, but this needs to be substantiated by experiments, so we next investigate the relationship between activation time of flow units and plastic deformation in MGs. We deformed $La_{75}Ni_{7.5}Al_{16}Co_{1.5}$ ribbons using the mandrel winding method with the same initial imposed strain of 0.943% and held the fully wound ribbons in place for different time t. We measured the curvature radius r and residual strain ε of these released ribbons after being held for different time spans (See Table S2 [28]). Figure 4(a) shows the ε change of these coiled ribbons with varied t. A ribbon which was fully wound and held for shorter t has a smaller ε as shown in the inset picture in Fig. 4(a). With increasing t, ε increases rapidly at the beginning, but the rate of increase of ε slows and approaches a saturation value of 0.635%. The changing tendency of ε with time t indicates the time dependent activation of the flow units in MGs [2,31,32]. Flow units with higher (lower) activation energy need a longer (shorter) time to be activated. Therefore, for the shorter deformation time, only the few flow units with lower E_{FU} can be activated and the ribbons correspondingly show small ε. With an extension of deformation time, more and more flow units with higher E_{FU} are activated, and the ribbons show larger ε. The flow units are found to correlate with some properties P such as elastic moduli of MGs in the form of [33] $P = P_m/(1 + c)$, where c correlates to the effective concentration of flow units, and P_m is the property of glass without flow units corresponding to that of perfect crystal [33]. We find that the formula of $\varepsilon(t) = \varepsilon_0/(1 + c)$ can fit the relationship of ε and t well, as shown in Fig. 4(a). The results clearly indicate that the plasticity of

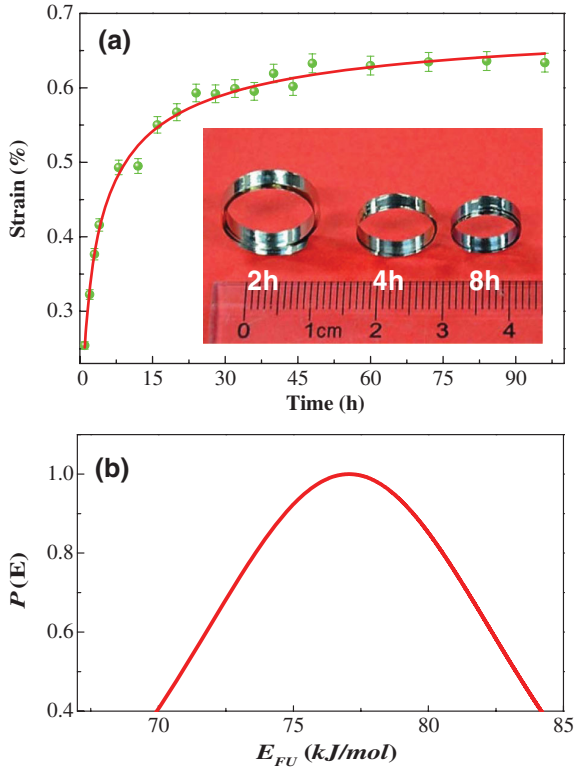

FIG. 4 (color). (a) The change in ε of $La_{75}Ni_{7.5}Al_{16}Co_{1.5}$ MG which was wound and held for different time spans. The inset shows an image of ribbons which were wound and then held in place for 2, 4 and 8 h, which have different curvature radii. The red curve is the fit using $\varepsilon(t) = \varepsilon_0/(1 + c)$. (b) The activation energy spectrum of the MG.

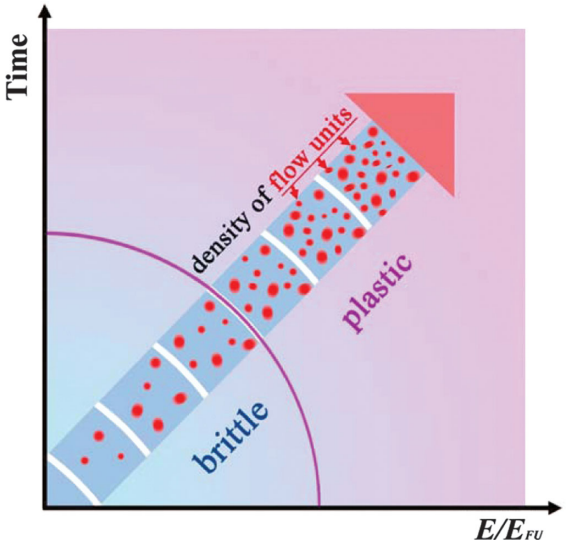

FIG. 5 (color). A schematic illustration of the relationship between flow units, applied external energy E (scaled by E_{FU}) and homogeneous plastic deformation in MGs. In the arrow the flow units are represented by the red regions in the blue elastic matrix, and the arrow indicates an increased tendency for flow unit density. The flow units percolate at a critical point (the purple percolation line), and lead to homogeneous deformation in MGs.

a MG is closely correlated with the density of the flow units and the deformation time.

We get the distribution of activation energy (or size) of flow units in MGs using the activation energy spectrum model [34]. The variation of ε on deformation time t and T can be expressed by the integral equation [34]:

$$\Delta\varepsilon(t) = \int_0^{+\infty} p(E)\theta(E,T,t)dE, \qquad (2)$$

where $\Delta\varepsilon(t) = \varepsilon_0 - \varepsilon(t)$, $\varepsilon(t)$ is the deformation time dependent strain, ε_0 is the saturation strain when t approaches infinity, $p(E)$ is the total available property change induced by all the activation processes in the range of E to $E + dE$, and $\theta(E,T,t) = 1 - \exp(-t/\tau) = 1 - \exp[-\upsilon_0 t \exp(E/kT)]$, is the characteristic annealing function; here, υ_0 is the Debye frequency 10^{13} s^{-1}. The E_{FU} has a broad distribution and only those flow units with $E_{FU} < E_c$ contribute to the relaxations or plasticity. E_c is the critical energy for activation of a flow unit. In the frame of steplike approximation, $p(E) = (\upsilon/kT)(d\varepsilon(t)/dlnt)$ and $E = kT\ln(\upsilon_0 t)$, we obtain the activation energy spectra of the flow units as shown in Fig. 4(b), where $P(E)$ is normalized by the value at the peak. The relation between the E_{FU} and size Ω of flow units can be estimated as [35] $E_{FU} = (8/\pi^2)G\gamma_c\zeta\Omega$, where G is the shear modulus, $\gamma_c \approx 0.027$ is the average elastic limit, and $\zeta \approx 3$ is a correction factor. The size distribution of flow units is then obtained [see Fig. S9 [28]]. The relaxation time τ spectra of the flow units can also be obtained based on the time dependent flow unit activation (see Fig. S10 [28]). The τ of flow units also has a broad distribution at RT, and only when the experimental time $t > \tau$ can the flow units be activated and contribute to the plastic deformation, which agrees with experimental observation [36].

From the above results, a diagram of the plastic deformation of a MG can be constructed based on the concept of flow unit, activation time t, and imposed energy E as illustrated in Fig. 5. The plasticity of a MG depending on E and the density of flow units connect with activation time and intensity of β relaxation. When the t is longer than the τ of flow units, which has a broad distribution in temporal scale [34], or high enough energy E is applied, greater numbers of flow units will be activated. As shown in Fig. 5, the MG then becomes plastic with an increase in t or E. When the density of flow units achieves a critical point, or $E > E_{FU}$, percolation of flow units occurs and leads to a homogeneous plastic deformation. The diagram implies that if the $t > \tau$ or if enough energy is applied to activate a sufficiently high density of flow units, then homogeneous plastic deformation can occur in any MG at RT depending on the activation, density, and percolation mode of flow units. The intrinsic microstructural origin for the plasticity of MG is related to the features of the flow units. Further

work with the mandrel winding approach can be extended for studying other fundamental issues such as structural origin of relaxations and aging of MGs.

Experimental assistance with D. Q. Zhao, D. W. Ding, M. Gao, Y. Z. Li, and Y. T. Sun are appreciated. This work was supported by the NSF of China (51271195) and MOST 973 of China (No. 2010CB731603).

*Corresponding author.hybai@iphy.ac.cn

[1] J. Schroers, Phys. Today **66**, No. 2, 32 (2013).
[2] W. H. Wang, Prog. Mater. Sci. **57**, 487 (2012).
[3] W. H. Peter, P. K. Liaw, R. A. Buchanan, C. T. Liu, C. R. Brooks, J. A. Horton, C. A. Carmichael, and J. L. Wright, Intermetallics **10**, 1125 (2002).
[4] M. D. Demetriou, M. E. Launey, G. Garrett, J. P. Schramm, D. C. Hofmann, W. L. Johnson, and R. O. Ritchie, Nat. Mater. **10**, 123 (2011).
[5] X. K. Xi, D. Zhao, M. Pan, W. Wang, Y. Wu, and J. Lewandowski, Phys. Rev. Lett. **94**, 125510 (2005).
[6] Y. H. Liu, G. Wang, R. J. Wang, D. Q. Zhao, M. X. Pan, and W. H. Wang, Science **315**, 1385 (2007).
[7] M. Chen, A. Inoue, W. Zhang, and T. Sakurai, Phys. Rev. Lett. **96**, 245502 (2006).
[8] J. Das, M. Tang, K. Kim, R. Theissmann, F. Baier, W. Wang, and J. Eckert, Phys. Rev. Lett. **94**, 205501 (2005).
[9] G. Kumar, T. Ohkubo, T. Mukai, and K. Hono, Scr. Mater. **57**, 173 (2007).
[10] H. B. Yu, X. Shen, Z. Wang, L. Gu, W. H. Wang, and H. Y. Bai, Phys. Rev. Lett. **108**, 015504 (2012).
[11] J. J. Lewandowski, W. H. Wang, and A. L. Greer, Philos. Mag. Lett. **85**, 77 (2005).
[12] G. Kumar, P. Neibecker, Y. H. Liu, and J. Schroers, Nat. Commun. **4**, 1536 (2013).
[13] P. Tandaiya, U. Ramamurty, G. Ravichandran, and R. Narasimhan, Acta Mater. **56**, 6077 (2008).
[14] A. S. Argon, Acta Metall. Mater. **27**, 47 (1979).
[15] S. T. Liu, Z. Wang, H. L. Peng, H. B. Yu, and W. H. Wang, Scr. Mater. **67**, 9 (2012).
[16] W. Dmowski, T. Iwashita, C. P. Chuang, J. Almer, and T. Egami, Phys. Rev. Lett. **105**, 205502 (2010).
[17] P. Y. Huang, S. Kurasch, J. S. Alden, A. Shekhawat, A. A. Alemi, P. L. McEuen, J. P. Sethna, U. Kaiser, and D. A. Muller, Science **342**, 224 (2013).
[18] Z. Wang, P. Wen, L. S. Huo, H. Y. Bai, and W. H. Wang, Appl. Phys. Lett. **101**, 121906 (2012).
[19] J. C. Ye, J. Lu, C. T. Liu, Q. Wang, and Y. Yang, Nat. Mater. **9**, 619 (2010).
[20] K. L. Ngai, P. Lunkenheimer, C. León, U. Schneider, R. Brand, and A. Loidl, J. Chem. Phys. **115**, 1405 (2001).
[21] R. Richert and K. Samwer, New J. Phys. **9**, 36 (2007).
[22] Y. Wu, X.-P. Tang, U. Geyer, R. Busch, and W. L. Johnson, Nature (London) **402**, 160 (1999).
[23] H. L. Peng, M. Z. Li, and W. H. Wang, Phys. Rev. Lett. **106**, 135503 (2011).
[24] J. S. Langer, Phys. Rev. E **77**, 021502 (2008).
[25] W. H. Wang, J. Appl. Phys. **110**, 053521 (2011).
[26] J. D. Ju, D. Jang, A. Nwankpa, and M. Atzmon, J. Appl. Phys. **109**, 053522 (2011).
[27] K. L. Ngai, L.-M. Wang, R. Liu, and W. H. Wang, J. Chem. Phys. **140**, 044511 (2014).
[28] See Supplemental Material at http://link.aps.org/supplemental/10.1103/PhysRevLett.113.045501 for experimental details, Tables S1–S2, Figs. S1–S10, and Refs. S1–S12.
[29] R. Casalini and C. M. Roland, Phys. Rev. Lett. **102**, 035701 (2009).
[30] O. Haruyama, Y. Nakayama, R. Wada, H. Tokunaga, J. Okada, T. Ishikawa, and Y. Yokoyama, Acta Mater. **58**, 1829 (2010).
[31] W. Jiao, B. A. Sun, P. Wen, H. Y. Bai, Q. P. Kong, and W. H. Wang, Appl. Phys. Lett. **103**, 081904 (2013).
[32] J. C. Dyre, Rev. Mod. Phys. **78**, 953 (2006).
[33] D. P. Wang, Z. G. Zhu, R. J. Xue, D. W. Ding, H. Y. Bai, and W. H. Wang, J. Appl. Phys. **114**, 173505 (2013); Z. G. Zhu, P. Wen, D. . Wang, R. J. Xue, D. Q. Zhao, and W. H. Wang, J. Appl. Phys. **114**, 083512 (2013).
[34] M. R. J. Gibbs, J. E. Evetts, and J. A. Leake, J. Mater. Sci. **18**, 278 (1983).
[35] W. L. Johnson and K. Samwer, Phys. Rev. Lett. **95**, 195501 (2005).
[36] W. Jiao, P. Wen, H. L. Peng, H. Y. Bai, B. A. Sun, and W. H. Wang, Appl. Phys. Lett. **102**, 101903 (2013).